

Dynamics of ammonia decomposition on Ru(0001)

H. Mortensen,^{a)} L. Diekhöner, A. Baurichter, E. Jensen, and A. C. Luntz

Fysisk Institut, University of Southern Denmark, Main Campus: Odense University, Campusvej 55, DK-5230 Odense M, Denmark

(Received 12 April 2000; accepted 26 July 2000)

Using supersonic molecular beam techniques we have investigated the dissociative adsorption of NH_3 on a Ru(0001) surface. At high incident energies, the dissociation increases substantially due to a direct breaking of the N–H bond on impact with the surface. For low incident translational energies, the dissociation depends on surface temperature T_s in an unusual manner, peaking sharply around 400 K. Increasing the surface defect density by low-fluence Ar^+ sputtering strongly enhances the dissociation probability while preserving the overall T_s -dependence. We interpret the low incident energy behavior as due to a mechanism in which a molecular precursor must undergo diffusion to defects before dissociating. At the lowest surface temperatures, dissociation is limited by the diffusion of the reaction products away from the defects in order to reactivate them. A kinetic model based on this mechanism is developed which is in good agreement with all experimental observations. © 2000 American Institute of Physics. [S0021-9606(00)70340-0]

I. INTRODUCTION

The synthesis of ammonia from N_2 and H_2 is one of the most important industrial catalytic processes. To date, the principal catalyst for this reaction has been based on reduced iron in the so called Haber–Bosch synthesis of NH_3 . In recent years, ruthenium has also been investigated as an end catalyst for NH_3 synthesis.¹ The motivation for this is that ruthenium has a higher activity than reduced iron, although it is also considerably more expensive. This recognition has led to an enormous effort in the surface science community over the past several years to understand all chemistry on ruthenium relevant to ammonia synthesis. In most surface science studies, the single crystal Ru(0001) surface has been used as the model catalyst.

It is generally accepted that for NH_3 synthesis, the rate limiting step in the process is the dissociative adsorption of N_2 . For Ru(0001), it has recently been shown that the barrier for N_2 dissociation on the single crystal terraces is very high (≥ 2 eV) and increases with the coverage of adsorbed N atoms.^{2,3} Recent experimental and theoretical work^{4,5} has also revealed that this barrier is substantially lowered at steps so that the reactivity of any real Ru(0001) sample surface, and certainly a catalyst surface, for dissociating N_2 is dominated by the number of available step/defect sites on the surface. Thus it is crucial to the catalysis that the steps or other active sites are not occupied by adsorbed species. Since catalysis is done in a partially closed system, decomposition of the product NH_3 , as well as the H_2 and N_2 , is important in determining surface coverages. For example, in the Haber–Bosch synthesis using reduced iron catalysts, the minimum temperature of the catalytic reactor is usually determined by the need to limit the surface N coverage which is determined by NH_3 dissociation.⁶ Using a higher temperature than re-

quired for the activated dissociation of N_2 in the catalysis raises the energy requirement, and thus the cost, of the catalytic process. In part, the advantage of Ru as a catalyst is that N poisoning of the catalyst is less severe due to a lower temperature for N_2 associative desorption. Ru can therefore be effectively utilized at higher NH_3 reactor pressures and/or lower reactor temperatures than Fe. It has recently been shown that the low temperature for nitrogen associative desorption from Ru(0001) is also critically dependent on available step sites.^{4,5} This underscores again the importance of surface poisoning of steps and defects in the catalysis by dissociation of the products as well as reactants in the catalysis. Thus, knowledge of the dissociative adsorption of NH_3 on Ru is required for a full understanding of Ru as an ammonia synthesis catalyst.

The adsorption of ammonia on Ru(0001) has been the object of several previous studies. Early thermal adsorption studies using AES (Auger electron spectroscopy) and LEED (low-energy electron diffraction) showed that at low surface temperatures (≈ 100 K) ammonia adsorbs molecularly with high probability on the Ru(0001) surface.⁷ Annealing the surface to desorb the NH_3 produced no dissociation.^{7,8} Temperature-programmed desorption (TPD) experiments were used to determine the desorption energy of the thus adsorbed molecules⁹ and the desorption energy at zero coverage was found to be $E_{\text{des}} = 0.93$ eV. At higher coverages additional desorption peaks at 180 K, 140 K, and 115 K were found, the first attributed to saturating a (2×2) adlayer, and the latter two corresponding to bi- and multilayer adsorption.

On Ru(0001) surfaces above room temperature the adsorption was found to occur dissociatively and with a low probability ($\leq 10^{-3}$)^{7,8,10} which depended significantly on surface temperature T_s . The dependence of the dissociation rate on T_s in the various studies was, however, inconsistent. Danielson *et al.*⁷ and Egawa *et al.*¹¹ showed a rather sharp peaking in the dissociation rates at $T_s = 450$ – 550 K, depending slightly upon exposure or pressure conditions at steady

^{a)} Author to whom correspondence should be addressed. Fax: +45 66158760; electronic mail: henrikm@fysik.sdu.dk

state, but falling an order of magnitude at both low and high surface temperatures. Danielson *et al.*⁷ focused upon the increase in dissociation with T_s in the region 300–400 K and discussed the dissociation in terms of an activated process. This does not, however, explain in any way the decrease in dissociation at higher T_s . On the other hand, Tsai and Weinberg¹⁰ found that the steady state decomposition rate of ammonia increased monotonically with T_s from 530 to 1250 K, albeit with different apparent activation energies below and above ≈ 750 K. This observation of an increase in NH_3 dissociation with T_s in this temperature region is in direct conflict with the previous observations. The activation energy for $T_s \leq 750$ K was suggested to be related to that for the associative desorption of nitrogen atoms from the surface. The lower activation energy at the higher T_s was attributed to the activated breaking of a N–H bond in a molecular precursor state. There is, thus, considerable inconsistency in both the experimental results and mechanistic interpretations for the dissociation of NH_3 on Ru(0001). It is, however, generally agreed that dissociation at low coverage does involve sequential dehydrogenation of the NH_3 followed by associative desorption of H_2 and N_2 if T_s is sufficiently high.

Egawa *et al.*¹¹ also studied dissociation on the stepped Ru(1,1,10) surface at $T_s \leq 630$ K. Both annealing the stepped surface with molecularly adsorbed NH_3 and steady state exposure to NH_3 gas yielded dissociation probabilities an order of magnitude larger than for the Ru(0001) surface. This certainly suggests that steps or defects may play a significant role in the dissociation mechanism on even the Ru(0001) surface. This concept is absent from previous discussions of the mechanism. This is a particularly relevant question with respect to Ru catalysts for NH_3 production since it has been inferred that these step/defect sites are the active sites in the catalysis.^{4,5}

All of the experiments mentioned above were performed at steady state or using large ammonia doses [several hundred langmuirs (L)]. It is thus not quite clear if the observed dependence of the reaction rate on surface temperature is related to the first dissociation step on the bare surface, or whether it merely reflects properties of the nitrogen desorption process. Given the observed influence of step sites in N_2 dissociation^{4,5} and also in associative desorption via detailed balance,⁴ it is certainly possible that the step/defect dependence observed for NH_3 dissociation is related to this later step.

In order to clarify the mechanism for NH_3 dissociation on Ru(0001) we have performed detailed molecular beam studies in an attempt to isolate the initial dissociative chemisorption step, i.e., the breaking of the first N–H bond. By using molecular beam techniques we are able to apply a well controlled, and yet quite low, dose of ammonia to the surface. In this way the interaction of an NH_3 molecule with the (almost) bare surface is studied. More importantly, supersonic molecular beam techniques allow the translational kinetic energy of the impinging molecules to be varied over a wide range, and thus probe specifically details of the dynamics of the first N–H bond breaking. Finally, T_s can be varied over a wide range as well. Variation of T_s and the translational energy of the NH_3 revealed that two “channels” exist

for the dissociative adsorption: a direct activated process and a molecular precursor mechanism. We find that the precursor-mediated dissociation depends strongly upon the number of surface defects. A kinetic model which includes diffusion to and poisoning of the defect sites by dissociation products reproduces the observed behavior of the precursor channel well, i.e., the unusual T_s dependence as well as the dependence on the number of defects.

II. EXPERIMENT

The experiments were carried out in a stainless steel ultrahigh vacuum (UHV) system previously described in detail.¹² The system has two identical triply differentially pumped supersonic molecular beam nozzles attached to the main UHV chamber which is equipped with standard tools for surface and gas analysis. The base pressure of this chamber is $\leq 1 \times 10^{-10}$ Torr. The nozzles had 75 μm diameter orifices. Due to the geometry of skimmers and apertures in the beam path, one beam had a diameter of ~ 2 mm at the sample while the other covered the entire sample surface. The small diameter beam could be modulated with a chopper wheel which allowed for the measurement of the translational energy of the molecules through their time-of-flight from the chopper to a rotatable Extrel quadrupole mass spectrometer (QMS) in the main chamber. The beam energy could be varied between 0.05 and 1.3 eV by varying the nozzle temperature between 300 K and 700 K and by seeding in H_2 , He, or Ar with various mixing ratios. It was assumed that the translational energy of the large area beam was identical to that measured for the small area beam since the nozzles were identical, gas mixtures identical, and nozzle temperatures were identical. Ammonia of 99.999% purity was used without further purification, as were the carrier gases H_2 (99.9997%), He (99.9999%), and Ar (99.9999%). During all adsorption measurements from either beam, the angle of incidence of the molecular beam was along the surface normal ($\theta_i = 0^\circ$).

A Ru(0001) crystal was mounted in a sample manipulator in the UHV chamber and cleaned as described previously.¹³ Structural defects were quantified by the relative magnitude of the defect peak in a TPD of a low dose (~ 0.02 L) of CO. This method showed a defect concentration of $\sim 0.25\%$. This indicates a very high quality Ru(0001) surface with a low step and defect density. The daily cleaning procedure consisted of sputtering followed by cycles of vacuum annealing to 1600 K and oxidation (by annealing to 1500 K in 5×10^{-8} Torr O_2). Surface carbon was removed by the oxidation. A final check for carbon contamination was then performed by monitoring CO temperature programmed desorption (TPD) after a 10 L O_2 dose. The surplus O_2 was desorbed by annealing to 1600 K. This latter procedure was also used to check for and remove any carbon buildup between repeated experiments. Contaminants other than carbon were monitored by Auger electron spectroscopy (AES). No surface impurities were detected during the course of the experiments.

The sample temperature was measured with a type C thermocouple fitted tightly into a hole in the side of the crystal and was ramped linearly for TPD measurements. TPD

spectra were recorded with the sample surface positioned 2 mm from the aperture of a conical cap isolating a differentially pumped UTi 100C QMS from the main chamber. This configuration minimized the signal from species desorbing from other places than the sample front surface. CO formed by C+O reaction as well as H₂ and N₂ formed statically by the molecular beam induced dissociation of NH₃ were recorded with a Balzers QMS-200 measuring partial pressures in the main chamber.

Relative NH₃ dissociative sticking coefficients (S) were measured in three different ways, applicable in different, partially overlapping surface temperature (T_s) regimes (1) ($300\text{ K} < T_s < 700\text{ K}$) In this regime, TPD of N₂ formed by associative desorption was measured after a small NH₃ molecular beam dose. For the NH₃ doses used in these experiments, the N₂ TPD was found to be proportional to the dose and hence the slope in a plot of the integrated TPD signal vs exposure is $\propto S$. TPD's were recorded at mass 28 to avoid the background signal at mass 14 resulting from residual NH₃. Since NH₃ does not molecularly adsorb to form a stable adlayer in this temperature regime, any sticking on the surface is due to dissociative adsorption breaking a N–H bond. Even though sticking for $T_s \leq 400\text{ K}$ does not fully dissociate NH₃ to yield adsorbed N, the subsequent anneal in the TPD dissociates fully all NH_x fragments produced in the original dissociative step. We note that no NH₃ associative desorption (formed by H+NH_x) was observed under any conditions. Thus, any initial dissociation breaking the first N–H bond irreversibly forms N₂ upon annealing. At temperatures above $\approx 700\text{ K}$, the N begins to slowly associatively desorb and is thus not stable on the surface for long times.

(2) ($T_s \geq 425\text{ K}$) In this region, the initial rise in H₂ partial pressure on dosing can be used as a monitor of S because adsorbed NH₃ dissociates completely to adsorbed N+H on Ru(0001)^{14–17} in this temperature regime. The hydrogen produced in the dissociation immediately desorbs and is used for quantifying the rate of dissociative adsorption. For $T_s \leq 400\text{ K}$ we find that not all the NH_x is fully dissociated nor is surface H fully desorbed,^{18,19} and thus this would be an unreliable method for measuring S .

(3) ($T_s \geq 1000\text{ K}$) At these temperatures, nitrogen produced by the dissociation of NH₃ rapidly recombines and desorbs as N₂. Thus the initial rise in N₂ partial pressure on dosing can be used as a measure of the initial dissociative sticking S .

The overlapping T_s regions of the three different methods were utilized to calibrate the relative sensitivities of each method relative to the others. An absolute calibration of the relative sticking coefficients was obtained by comparing these to a measurement via the King and Wells method²⁰ using a movable quartz flag to rapidly expose a clean surface. This method was only possible under conditions of the highest sticking, i.e., by increasing the defect concentration on the surface artificially, so that an absolute normalization was made for the defect system and all relative measurements were scaled to this measurement. For the deliberate introduction of additional surface defects sputtering by 1 keV Ar⁺ for 40 s at an ion current of $\sim 0.04\ \mu\text{A}$ was used.

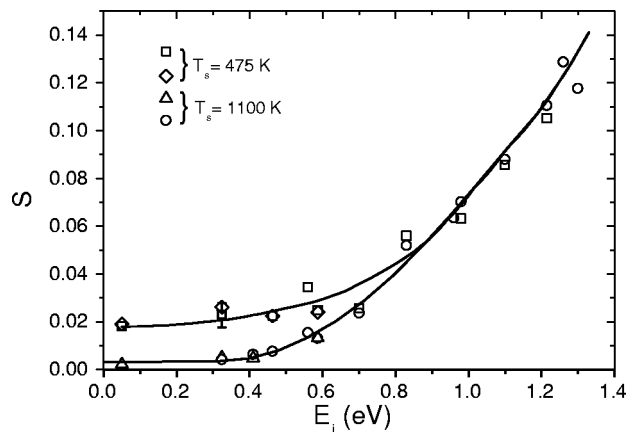


FIG. 1. The initial sticking coefficient as a function of the experimentally determined translational energy, E_i , of the ammonia molecules all incident along the surface normal. \square and \diamond denote dosing at a sample surface temperature $T_s = 475\text{ K}$, \triangle and \circ $T_s = 1100\text{ K}$. The detection methods were for \square : N₂ TPD; \diamond and \triangle : immediate H₂ desorption; \circ : immediate N₂ desorption. The lines for the two different T_s are merely drawn to guide the eye.

III. RESULTS AND DISCUSSION

The dependence of sticking on incident translational energy (E_i) for $\theta_i = 0^\circ$ was investigated by varying the nozzle temperature between 300 K and 700 K and by seeding the NH₃ in Ar, He, or H₂. The results are shown in Fig. 1 for two different surface temperatures $T_s = 475\text{ K}$ and $T_s = 1100\text{ K}$. At both temperatures, sticking grows substantially with incident translational energy for $E_i \geq 0.5\text{ eV}$. At high energies, the surface temperature seems to play only a minor role, if any at all. We interpret these two facts as indications that the NH₃ dissociation in this range of incident energy is limited by a direct activated dissociation process breaking a single N–H bond. Indeed, both the increase with E_i and the relative insensitivity to surface temperature are the principal features of a direct activated process. The former indicates that there is a barrier to reaction while the latter indicates no thermal equilibration with the surface before dissociation, i.e., that it is a direct process. The adiabatic (minimum energy path) barrier for the direct dissociation is *ca.* 0.5 eV. The accuracy of the data does not allow us to determine whether there is still a small T_s dependence of the sticking at high E_i , as has been observed for CH₄ dissociations.²¹

As further evidence that the dissociation of NH₃ at high incident energies is a direct activated dissociation, we have measured the incident angular dependence of the dissociation probability at $E_i = 1.1\text{ eV}$, $S(\theta_i, E_i = 1.1\text{ eV})$. We find that $S(\theta_i, E_i = 1.1\text{ eV})$ is peaked about the surface normal with an approximately $\cos^4\theta_i$ dependence. Dissociation probabilities which strongly peak about normal incidence are also a hallmark of most activated direct dissociations in which normal translational energy plays a role in surmounting the barrier. On the other hand, when molecules stick in highly laterally and rotationally corrugated molecular wells such as anticipated for NH₃/Ru, the sticking is nearly independent of the angle of incidence.²² Thus, $S(\theta_i, E_i = 1.1\text{ eV})$ is also inconsistent with a precursor mechanism.

At lower E_i sticking clearly depends on surface tempera-

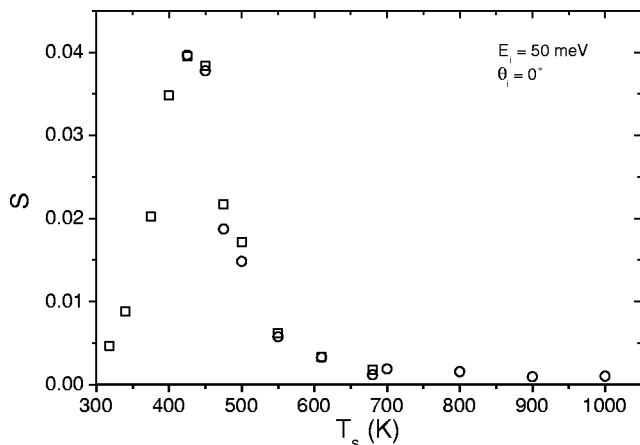


FIG. 2. S for NH_3 at $E_i = 50$ meV, normal incidence, vs surface temperature. \square are based on the N_2 TPD method; \circ on the immediate H_2 desorption.

ture, whereas the dependence on incident energy is very weak. This implies that the path to dissociation includes a molecular precursor state on the surface, in which the reactant thermally equilibrates with the surface and loses information on its incident energy. Precursor-mediated processes generally exhibit a decrease in S with E_i due to a fall off in trapping into the precursor well with incident energy. However, if molecular NH_3 is the precursor, then this fall is anticipated to be minimal since the well depth of the precursor is quite large (*ca.* 0.9 eV) and probably strongly laterally and orientationally corrugated.²²

In order to investigate the details of the low incident energy dissociation mechanism, the sticking of ~ 50 meV NH_3 was measured for various surface temperatures ranging from room temperature to 1000 K (see Fig. 2). The behavior at $T_s > 450$ K agrees qualitatively with a standard precursor-mediated process in which the reaction is turned off at high T_s due to thermal desorption from the precursor state, *i.e.*, where the barrier to dissociation is lower than that for desorption (and the phase space for dissociation is smaller than that for desorption). This does not, however, explain the decrease of S at lower T_s .

This co-existence of a direct activated process and a precursor-mediated one where the barrier to dissociation is less than the molecular desorption energy (the minimal incident energy of gas phase NH_3) is a contradiction in terms of a simple one dimensional picture of dissociation. Nevertheless, this dichotomy has been observed several times before. In some carefully studied systems, *e.g.*, neopentane²³ and methanol²⁴ on Pt(111) and ethane on Ir(111),²⁵ it has been shown that the precursor channel is dominated by dissociation at surface steps or defects while the activated direct process is dominated by dissociation at the terraces.

In the present case, the sticking coefficient peaks at $T_s \approx 400$ K and falls off quite rapidly as T_s is decreased below this maximum. This behavior cannot be explained by any simple precursor mechanism, whether at defects or on terraces, and suggests that at low T_s a third process is rate limiting. An obvious candidate is surface diffusion of trapped NH_3 to specific reactive sites (defects) and/or diffusion of reaction products away from these specific reactive

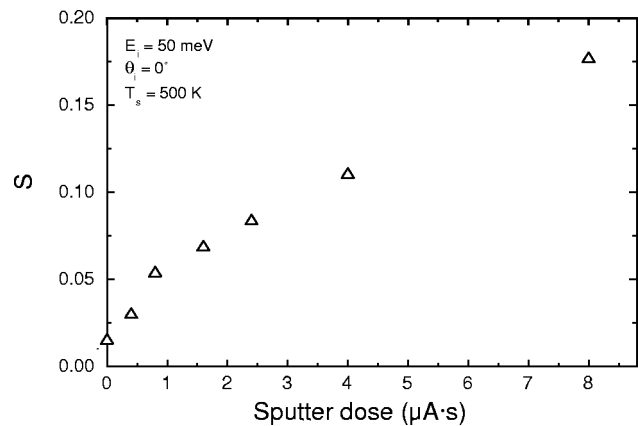


FIG. 3. S of NH_3 at $E_i \approx 50$ meV, normal incidence at a surface prepared by subjecting it to various doses of 1 keV Ar^+ ions. The sample was sputtered at room temperature. Sticking was measured by the immediate H_2 desorption from the 500 K surface at impact of the beam of NH_3 seeded in Ar.

sites. The latter is a necessary process to reactivate the “blocked” reactive sites in order for additional precursors to dissociate.

Further experiments were performed to clarify whether special sites, *i.e.*, defects, play a role in the reactivity of the Ru(0001) surface. By light Ar^+ sputtering, varying amounts of surface defects were introduced. The effect on the sticking of low energy ($E_i \approx 50$ meV) NH_3 at $T_s = 500$ K is shown in Fig. 3. These data very clearly show that surface defects created by sputtering strongly enhance the reactivity of the surface. In fact, assuming the defect density is linear with sputter dose, the approximate linear increase in S with sputter dose suggests that defects are entirely responsible for the low-energy dissociation. The dependence of the sticking on T_s after a fixed, moderate sputter dose of 1.6 $\mu\text{A s}$ corresponding to ~ 0.01 Ar^+ ions/surface atom, is shown in Fig. 4. Assuming a sputter yield of 1.7 for this incident energy²⁶ corresponds to creating a defect density of 1.7%. This agrees approximately with the total surface defect density estimated by CO titration of the defects after sputtering. It is evident in

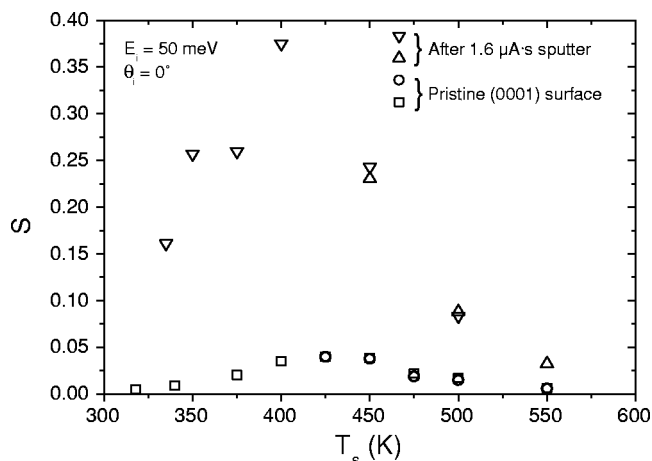


FIG. 4. A comparison of S of NH_3 at $E_i \approx 50$ meV and normal incidence as a function of surface temperature for the bare surface and a lightly sputtered surface. The detection methods were for ∇ and \square : N_2 TPD; \triangle and \circ : immediate H_2 desorption.

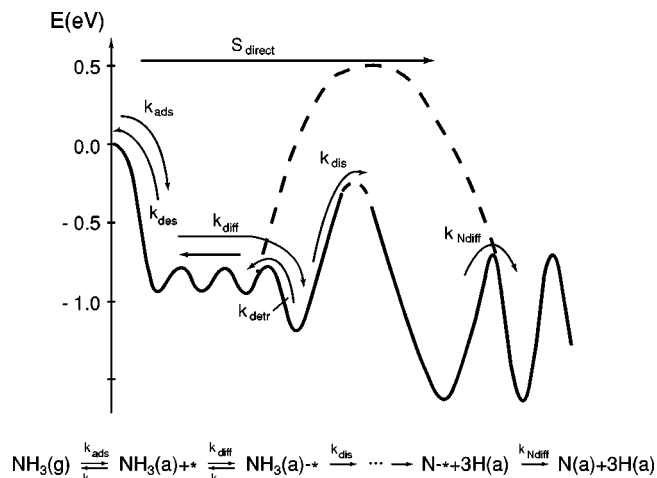
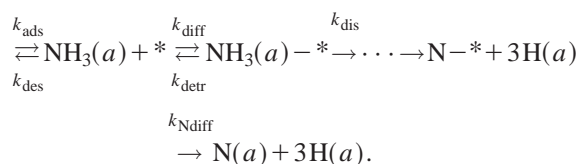
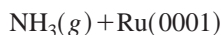


FIG. 5. The potential energy surface sketched as a function of the reaction coordinate for our model of the dissociative chemisorption of NH_3 on the Ru(0001) surface. In the precursor-mediated pathway, the molecule is trapped on a terrace, diffuses to a defect site and dissociates essentially leaving at the defect a nitrogen atom which finally diffuses away to reactivate the site. The dashed line indicates the barrier to direct dissociation.

Fig. 4 that the general temperature dependence of S is preserved relative to that of the original surface, but that S increases by approximately an order of magnitude due to generation of defects of *ca.* 1.7%. In summary, these experiments demonstrate that defects do dominate dissociation via a precursor mechanism. This conclusion is also consistent with previous thermal background experiments which demonstrated a much higher reactivity of the stepped Ru(1,1,10) surface relative to that of the Ru(0001) surface.¹¹

In order to understand the unusual T_s dependence and the role of defects in determining S in the precursor-mediated dissociation process, we have constructed a simple kinetic model. This model is based on the following kinetic equations and is sketched schematically in Fig. 5,



Here $\text{NH}_3(\text{g})$ is gas phase ammonia, $\text{NH}_3(\text{a})$ is adsorbed molecular ammonia, $*$ refers to the active defect site, $\text{NH}_3(\text{a})-*$ is molecular ammonia trapped at a defect site, N-* refers to products trapped at the defect site, and $\text{N}(\text{a})$ refers to the final product of the reaction (before associative desorption). This model includes the following kinetic steps: Adsorption of molecular ammonia (k_{ads}), thermal desorption of the molecularly adsorbed ammonia (k_{des}), diffusion of molecularly adsorbed ammonia to a defect site where it is trapped (k_{diff}), thermally induced de-trapping of the adsorbed ammonia from the defect site (k_{detr}), breaking of the first N–H bond or possibly several N–H bonds at the defect site (k_{dis}) and diffusion of N-containing dissociation product (possibly a N atom) far enough away from the defect site to reactivate it (k_{Ndiff}). Neglect of any reversible kinetic steps

TABLE I. The values of Arrhenius pre-exponential factors and activation energies used in the kinetic equations to model the observed dissociative adsorption process. The results of solving the equations using these parameters are shown in Fig. 6.

Step (j)	A_j (s^{-1})	E_j (eV)
NH_3 desorption (des)	10^{13}	0.93
NH_3 diffusion (diff)	10^{13}	0.15
NH_3 detrapping (detr)	10^{13}	0.40
Dissociation (dis)	10^{12}	0.91
Product diffusion (Ndiff)	10^{13}	0.94

after the breaking of the initial N–H bond is justified by the lack of any observable NH_x formed by associative desorption from any NH_x fragments. Removal of the hydrogen produced is assumed to occur rapidly and is not included explicitly in the model.

Based on the model outlined above, a set of coupled kinetic equations describes the overall concentrations of all 5 surface species [$\text{NH}_3(\text{a})$, $*$, $\text{NH}_3(\text{a})-*$, N-* , and $\text{N}(\text{a})$]. We assume that the rate of each kinetic step can be described by an Arrhenius rate $k_j = A_j \exp(-E_j/k_B T) \Pi \theta_{\text{reactant}}$, where E_j is the activation energy of step j , A_j is the usual Arrhenius pre-exponential, and $\Pi \theta_{\text{reactant}}$ is the product of the coverages of the reactants of the step j . All kinetic steps were thus assumed to follow the obvious reaction orders. The coupled kinetic equations were solved numerically for the surface concentrations of all species. The parameters used in the model are given in Table I. There is good evidence for some of these from the literature; $E_{\text{des}} = 0.93$ eV,⁹ $E_{\text{diff}} \approx 0.15$ eV from laser measurements of NH_3 diffusion on Re(0001),²⁷ and $E_{\text{Ndiff}} = 0.94$ eV.²⁸ For the latter, we assume that diffusion of N or other product away from the defect is the same as N diffusion on the bare surface. For most of the others we have simply assumed fixed reasonable values, i.e., Arrhenius pre-exponentials of 10^{13} s^{-1} , etc. In order to achieve reasonable qualitative agreement with the experimental results, we have varied E_{detr} , E_{dis} , and A_{dis} .

The results of numerically solving the kinetic equations and integrating the reaction product to a time similar to our dosing time are shown in Fig. 6. Sticking was calculated for defect densities of 0.2% and 2.0%, corresponding roughly to the experimental conditions of a clean and a sputtered surface, respectively. In Fig. 2, the decrease in T_s above 450 K is due to the fact that the effective desorption energy from defect sites ($E_{\text{detr}} - E_{\text{diff}} + E_{\text{des}}$) $> E_{\text{dis}}$ and $A_{\text{dis}} < A_{\text{des}}$, similar to a conventional precursor-mediated mechanism. The decrease in S at $T_s < 450$ K is due to poisoning of the defect sites by limited diffusion of reaction product away from them at the lower T_s .

A comparison of Figs. 4 and 6 clearly shows a qualitative and approximate quantitative agreement between the experiment and the model calculation. However, since there are so many unknown parameters in this kinetic model, this agreement should in no way be interpreted as “proof” of the model nor of an experimental determination of unknown parameters. It should rather be concluded that the model is fully consistent with all experimental results.

The experimental results obtained here, and the interpre-

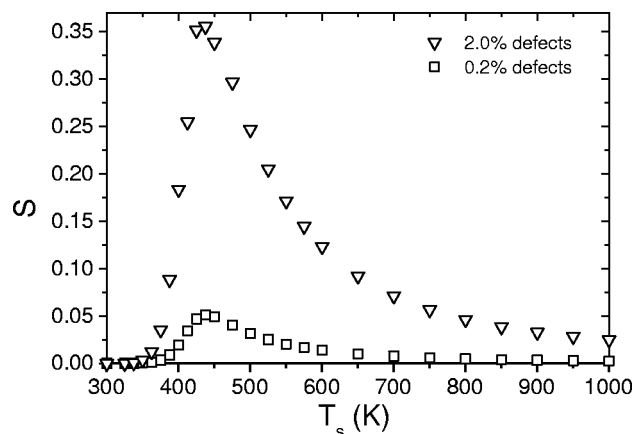


FIG. 6. Model calculations of the sticking coefficient vs surface temperature based on the model potential energy diagram in Fig. 5. The sticking was calculated for two surface defect densities: 0.2% (\square), corresponding to our clean Ru(0001) surface, and 2.0% (∇), corresponding to a lightly sputtered surface (cf. Fig. 4).

tation of them, are in good agreement with the prior large or steady state exposure experiments of Danielson *et al.*⁷ and Egawa *et al.*,¹¹ including the increased dissociation via stepped surfaces. Our experimental results and interpretation, however, are in conflict with the T_s dependence of rates obtained in the steady-state experiments of Tsai and Weinberg.¹⁰ They interpreted their results as an increase in the dissociation rate with T_s and proposed that overall dissociation was limited by activated dissociation by a molecular precursor ($T_s > 750$ K) or by associative desorption of N_2 ($T_s < 750$ K). We will not try to reconcile their experiments with ours since we have no way to judge the validity of their experimental results nor their analysis. We do note, however, that if the defects are completely and irreversibly poisoned in our model, then the remaining mechanism becomes equivalent to an activated molecular-precursor mechanism (plus the direct dissociation).

The finding here that steps/defects dominate the dissociation of low incident energy NH_3 on the nominally low defect Ru(0001) surface suggests that this mechanism must certainly dominate for any real catalyst. Thus, not only are the defect sites important in lowering the barrier for N_2 dissociation^{4,5} but also in determining the ultimate surface coverages through reverse dissociation of the products.

IV. CONCLUSIONS

Using supersonic molecular beam techniques we have shown that two pathways exist for the dissociative adsorption of ammonia on Ru(0001). At high incident energy the dissociative adsorption occurs via a direct activated process since it shows a strong increase with incident energy and little or no dependence on surface temperature. The adiabatic or minimum barrier height is *ca.* 0.5 eV. On the other hand, at low incident energy, the reaction yield depends principally on surface temperature and suggests that a precursor-mediated process is involved. However, in conflict with a simple precursor-mediated mechanism, the T_s dependence is complex and the dissociation peaks rather sharply at *ca.* $T_s = 400$ K at fairly low values of *ca.* 10^{-2} , decreasing both

above and below this T_s . Since light sputtering increases the magnitude of the dissociation almost linearly with the sputter dose, a role for surface defects in the precursor dissociation is suggested. We propose that the mechanism is dominated by diffusion of molecularly adsorbed NH_3 to and diffusion of reaction products away from defect sites, which are the active ones for the dissociation. It is suggested that the decrease of S with T_s above 400 K is due to that normally associated with a molecular precursor (competition of desorption vs. dissociation) while the decrease of S below 400 K is due to “blocking” of the active defect sites due to limited diffusion of reaction products away from those sites. A kinetic model of the reaction based on this mechanism and known or reasonable kinetic parameters gives good qualitative agreement with the experimental results for two different surface defect densities.

ACKNOWLEDGMENTS

The authors gratefully acknowledge the Danish Research Council for partial support of this work under Grant No. 9601724. H.M. and L.D. also wish to thank the Danish Research Academy for supporting their Ph.D. studies.

- ¹S. R. Tennison, in *Catalytic Ammonia Synthesis: Fundamentals and Practice*, edited by J. R. Jennings (Plenum, New York, 1991), Chap. 9, pp. 303–364.
- ²L. Diekhöner, H. Mortensen, A. Baurichter, and A. C. Luntz, *J. Vac. Sci. Technol. A* **18**, 1509 (2000).
- ³L. Diekhöner, H. Mortensen, A. Baurichter *et al.*, *Phys. Rev. Lett.* **84**, 4906 (2000).
- ⁴S. Dahl, R. C. Egeberg, J. H. Larsen *et al.*, *Phys. Rev. Lett.* **83**, 1814 (1999).
- ⁵S. Dahl, E. Törnqvist, and I. Chorkendorff, *J. Catal.* **192**, 381 (2000).
- ⁶P. Stoltze, *Phys. Scr.* **36**, 824 (1987).
- ⁷L. Danielson, M. Dresser, E. Donaldson, and J. Dickinson, *Surf. Sci.* **71**, 599 (1978).
- ⁸C. Egawa, S. Naito, and K. Tamaru, *Surf. Sci.* **138**, 279 (1984).
- ⁹C. Benndorf and T. E. Madey, *Surf. Sci.* **135**, 164 (1983).
- ¹⁰W. Tsai and W. H. Weinberg, *J. Phys. Chem.* **91**, 5302 (1987).
- ¹¹C. Egawa, T. Nishida, S. Naito, and K. Tamaru, *J. Chem. Soc., Faraday Trans. 1* **80**, 1595 (1984).
- ¹²A. C. Luntz, M. D. Williams, and D. S. Bethune, *J. Chem. Phys.* **89**, 4381 (1988).
- ¹³L. Diekhöner, A. Baurichter, H. Mortensen, and A. C. Luntz, *J. Chem. Phys.* **112**, 2507 (2000).
- ¹⁴H. Rauscher, K. L. Kostov, and D. Menzel, *Chem. Phys.* **177**, 473 (1993).
- ¹⁵H. Dietrich, K. Jacobi, and G. Ertl, *J. Chem. Phys.* **105**, 8944 (1996).
- ¹⁶H. Dietrich, K. Jacobi, and G. Ertl, *Surf. Sci.* **377–379**, 308 (1997).
- ¹⁷C. J. Hagedorn, M. J. Weiss, and W. H. Weinberg, *J. Vac. Sci. Technol. A* **16**, 984 (1998).
- ¹⁸P. Feulner and D. Menzel, *Surf. Sci.* **154**, 465 (1985).
- ¹⁹T. A. Jachimowski, B. Meng, D. F. Johnson, and W. H. Weinberg, *J. Vac. Sci. Technol. A* **13**, 1564 (1995).
- ²⁰D. A. King and M. G. Wells, *Surf. Sci.* **29**, 454 (1972).
- ²¹A. C. Luntz and J. Harris, *Surf. Sci.* **258**, 397 (1991).
- ²²J. Harris and A. C. Luntz, *J. Chem. Phys.* **91**, 6421 (1989).
- ²³J. F. Weaver, M. A. Krzyzowski, and R. J. Madix, *Surf. Sci.* **393**, 150 (1997).
- ²⁴L. Diekhöner, D. A. Butler, A. Baurichter, and A. C. Luntz, *Surf. Sci.* **409**, 384 (1998).
- ²⁵D. F. Johnson and W. H. Weinberg, *J. Chem. Phys.* **101**, 6289 (1994).
- ²⁶N. Matsunami, Y. Yamamura, Y. Itikawa *et al.*, *At. Data Nucl. Data Tables* **31**, 1 (1984).
- ²⁷I. Farbman, Z. Rosenzweig, and M. Asscher, *Faraday Discuss.* **96**, 307 (1993).
- ²⁸T. Zambelli, J. Trost, J. Winterlin, and G. Ertl, *Phys. Rev. Lett.* **76**, 795 (1996).